Small-scale structure of the disc velocity distribution. A maximum entropy statistical approach - Part II

Rafael Cubarsi

Dept. Matemàtica Aplicada IV
Universitat Politècnica de Catalunya
08034 Barcelona, Catalonia, Spain
E-mail:rcubarsi@ma4.upc.edu

December 2009

Abstract

Among metallicity, colour, and other star properties, the eccentricity of the star's orbit behaves as a very good sampling parameter to find a more detailed structure for the disc velocity distribution, allowing distinctions between different eccentricity layers. For subsamples with eccentricities $e < 0.15$, star velocities are approximately symmetrically distributed around the LSR in the radial direction, with a dearth of stars at the LSR. For $e = 0.15$, the core distribution of the thin disc is supported by two major stellar groups with opposite radial velocities. Several simulations confirm that such a double-peaked distribution comes from the lognormal distribution of the velocity amplitudes. For maximum eccentricity 0.3 and maximum distance to the Galactic plane 0.5 kpc a representative thin disc sample is obtained. An explanation of the apparent vertex deviation of the disc from the swinging of those major kinematic groups around the LSR is possible, which predicts a continuously changing orientation of the disc's pseudo ellipsoid.

KEY WORDS: stars: kinematics – galaxies: kinematics and dynamics – galaxies: statistics – methods: statistical.
1991 MATHEMATICS SUBJECT CLASSIFICATION: 60, 62, 85.

1 Introduction

In Cubarsi (2008, 2009) the maximum entropy approach was used to describe the basic structure of the disc velocity distribution by working from complete and bounded stellar samples of the Geneva-Copenhagen survey (GCS) catalogue (Nordström et al 2004). It is however possible to obtain a more detailed shape for the velocity distribution for specific subsamples, allowing comparison of the results of our approach with the small-scale structure sustained by moving groups as described by other authors. By selecting samples with bounded peculiar velocity, such as $|\mathbf{u}| \leq 7.5$ km s^{-1} (256 stars), 10 km s^{-1} (498 stars), or 20 km s^{-1} (2,817 stars), a more complex structure is manifest on the UV plane, but also in the vertical direction. The shape of the distribution becomes softer while increasing the size of the sample. Because of this, the substructure of thin disc subsamples with less stars become statistical fluctuations within larger subsamples, up to describing a sufficiently complete distribution of the thin disc. Thus the clue is to find a clean and representative thin disc sample. The cut $|\mathbf{V}| \leq 51$ km s^{-1} therefore seems to be a good value that includes most of thin disc stars and excludes thick disc stars, but it is still far from being a complete thin disc sample. Samples selected from small peculiar velocities have some limitations. On one hand, they contain few stars, so that their distribution may not be bell-shaped enough. Furthermore, their moments have greater uncertainties. On the other hand, the boundary of the distribution is fixed by the velocity limit of the sample, which may cut down some well-defined structures. Fortunately, there is a way to avoid this problem. In Alcobé & Cubarsi (2005) (hereafter Paper I) and Cubarsi et al. (2009) (hereafter Parer II), consecutive stellar populations were merged to nested subsamples in terms of several sampling parameters: maximum absolute velocity, peculiar velocity, vertical velocity, etc. Optimal values of these sampling parameters allowed the segregation of these populations. For the complete GCS sample, once the stars are classified according to the probability of belonging to any of the local Galactic components (Paper II), a highly significative correlation is obtained between the expected population of a star and its absolute velocity $|\mathbf{V}|$. The expected value is similarly highly correlated with the planar eccentricity, and also correlated with rotation velocity, $|z_{max}|$ and metallicity. The colour is few correlated with the expected population and the other preceding properties. Therefore significant partial correlations between couples of the former star properties exist. However, when the sample is bounded to $|\mathbf{V}| \leq 51$ km s^{-1}, by leaving aside thick disc and halo stars, the only significant partial correlation that is maintained is the absolute velocity and the eccentricity, as well as the expected population with them. That means that the other properties are only relevant for segregating thick-disc or halo stars, but are not useful within the very thin disc. As discussed in Paper II, the sampling parameter is related to the isolating integrals of the star motion. Both the absolute velocity and the eccentricity satisfy this requirement. The former is less discriminant, but is a direct measure from the star. The latter is more discriminant, but requires computing the orbital parameters, with the need of additional hypothesis on the potential, symmetries, stationarity, mean motion, solar position, etc. Therefore, it is possible to use the eccentricity not for segregating populations, as e.g., Pauli et al. (2005) or Vidojević & Ninković (2009), but as an improved sampling parameter to select subsamples.

2 Orbital eccentricity

For samples with maximum eccentricities 0.01 (220 stars), 0.02 (591 stars), 0.03 (1,058 stars), 0.05 (2,465 stars), 0.1 (7,095 stars), 0.15 (9,545 stars), 0.2 (10,903 stars), and 0.3 (11,826 stars), with the additional condition $|z_{\max}| < 0.5$ kpc to avoid contamination from stars not belonging

to the thin disc, the maximum entropy approach provides the series of plots in Figures 1, 2, 3, and 4. Both previous limitations introduced by the peculiar velocity boundary have disappeared. For example, the structure described by the plot $|\mathbf{u}| \leq 10$ km s^{-1} with 498 stars is now more completely described from the plot with maximum eccentricity 0.05 with 2,465 stars. Similarly, the shape of the distribution is no longer forced by the sampling parameter. The eccentricity then behaves as a very good sampling parameter that allows us to distinguish between different *eccentricity layers* within the thin disc and enables us to visualise the structure below each layer. In the lower layers, with maximum eccentricities 0.01 and 0.02, the velocity distribution shows a hole around the local standard of rest (LSR), taken as $(-10., -5.23, 7.17)$ km s^{-1} (Dehnen & Binney 1998), which is the mean of the distribution. Those lowest eccentricity stars are moving around the LSR and have velocities distributed on a ring with some peaks around the LSR. The radial velocities are symmetrically grouped into two main bulks at each side of the LSR. This behaviour is maintained up to eccentricity e=0.03, where the LSR hole begins to be filled by the group of stars corresponding to the Coma Berenices moving group, nearly at the same LSR velocity. In addition, three stellar groups around the LSR conform the basic structure: NGC 1901, a group that can be part of the middle branch (Skuljan et al. 1999), and a part of the Pleiades group. The structure is the same as described by Bovy et al. (2009) and by previous works of Dehnen (1998), Skuljan et al. (1999), Famaey et al. (2005, 2007), with the greatest peak in NGC 1901.

For e=0.05 the structure is maintained and enlarged. It incorporates a new group of stars also associated with the middle branch, which is not referred to as a moving group by Bovy et al. (2009), but is the centre of their Gaussian component with the largest weight. In the range of eccentricities from 0.05 to 0.1, the small previous structures are diluted in a background distribution, and only the Pleiades group remains. The main weight of the distribution is now in the stars around the Hyades group. A stellar group around the Sirius/UMa stream arises at positive radial velocities. For e=0.15, that is, approximately the higher eccentricity before appearing thick disc stars, the distribution is divided into about half: one bulk with negative radial and rotation mean velocities with respect to the LSR, which contain the main groups Hyades and Pleiades; and another one with positive values around Sirius and UMa stream. For higher eccentricities, the distribution becomes similar to the one corresponding to the thin disc. In particular, for e=0.3, with a fraction of 90% of the whole sample, we get a distribution similar to the thin disc of Paper II (obtained by two different methods: MEMPHIS algorithm and the method of Galactic orbits), with dispersions and vertex deviation $(\sigma_U, \sigma_V, \sigma_W; \delta)$=$(29.1 \pm 0.2, 18.1 \pm 0.1, 11.6 \pm 0.1; 10^\circ \pm 1)$.

Thus, for eccentricities below 0.15, there is a general trend in the radial direction: the main weight of the distribution is symmetrically placed around the LSR. Thus, the velocity distribution of the thin disc is supported by two major stellar groups with opposite radial velocities around the LSR, with a dearth of stars at the LSR. One bulk, with positive radial velocity, has a mean velocity similar to the Sun or slightly higher, with a lower peak but a wider distribution. The other one, with radial velocity ≈ -30 km s^{-1}, has a mean rotation ≈ -20 km s^{-1} and a higher peak. This behaviour is definitively broken for eccentricities $e \geq 0.2$.

3 Simulations

The situation described in the preceding section, where the star velocities are distributed for low eccentricities along the U direction with a local minimum at the LSR velocity, may have a simple explanation: a mixture of stars with a discrete number of radial oscillation periods. In the special case of a nearly planar orbit, where the planar eccentricity is low enough that the amplitude of

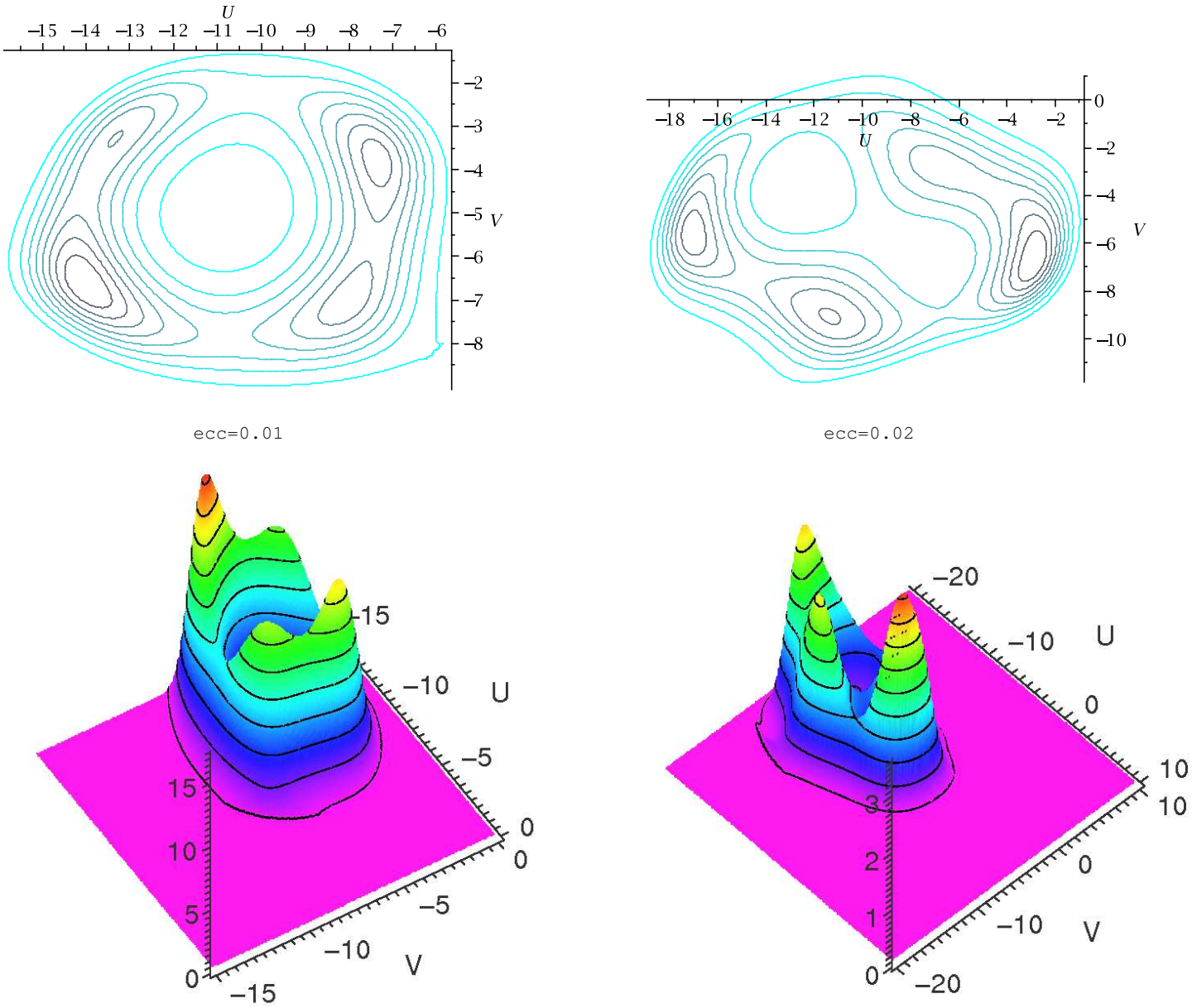

Figure 1: Series of contour plots and distributions on the UV plane for GCS subsamples selected from $|z_{\max}| < 0.5$ kpc and eccentricities up to 0.01 and 0.02. The origin is at the Solar velocity.

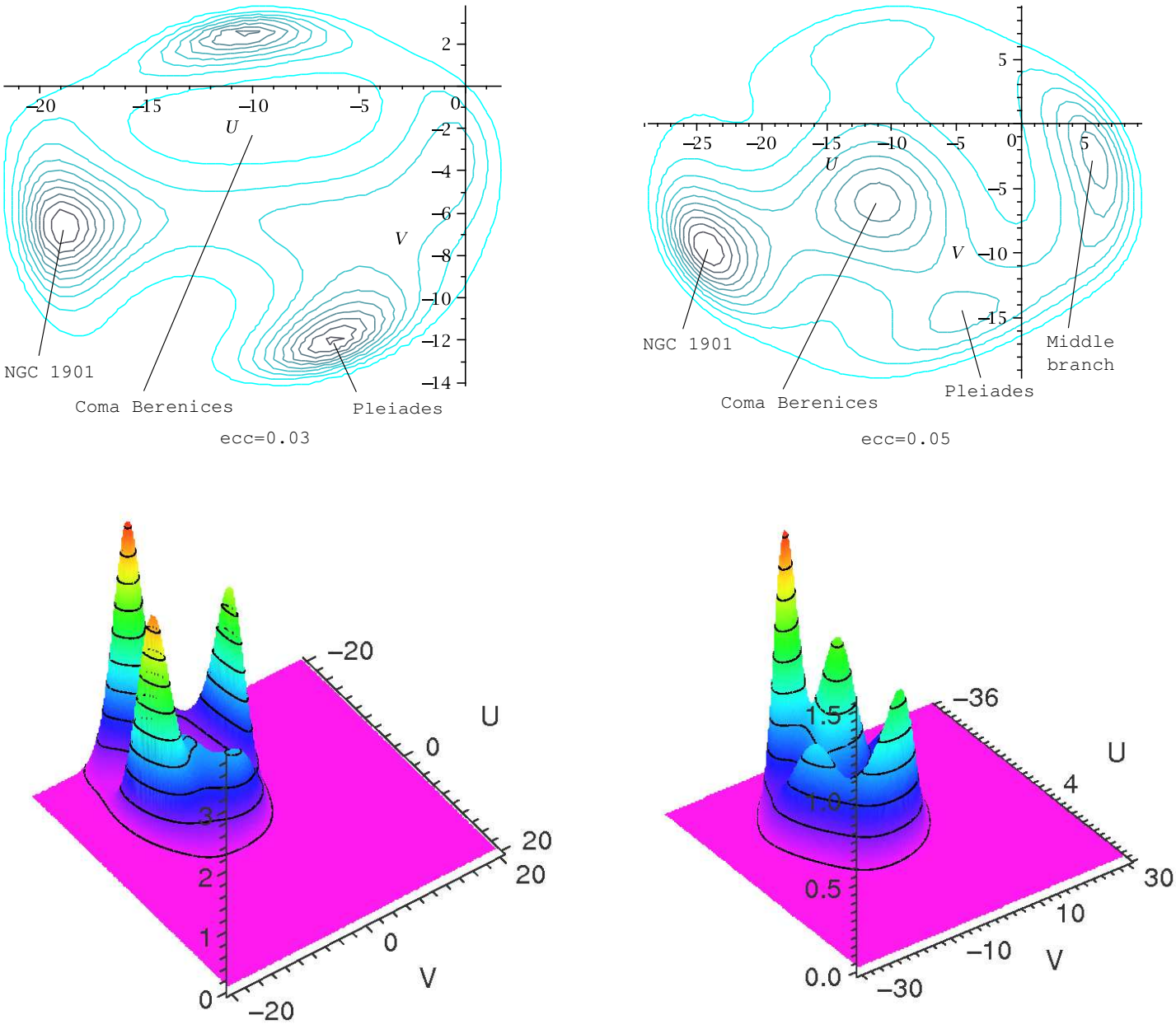

Figure 2: Series of contour plots and distributions on the UV plane for GCS subsamples selected from $|z_{\max}| < 0.5$ kpc and eccentricities up to 0.03 and 0.05.

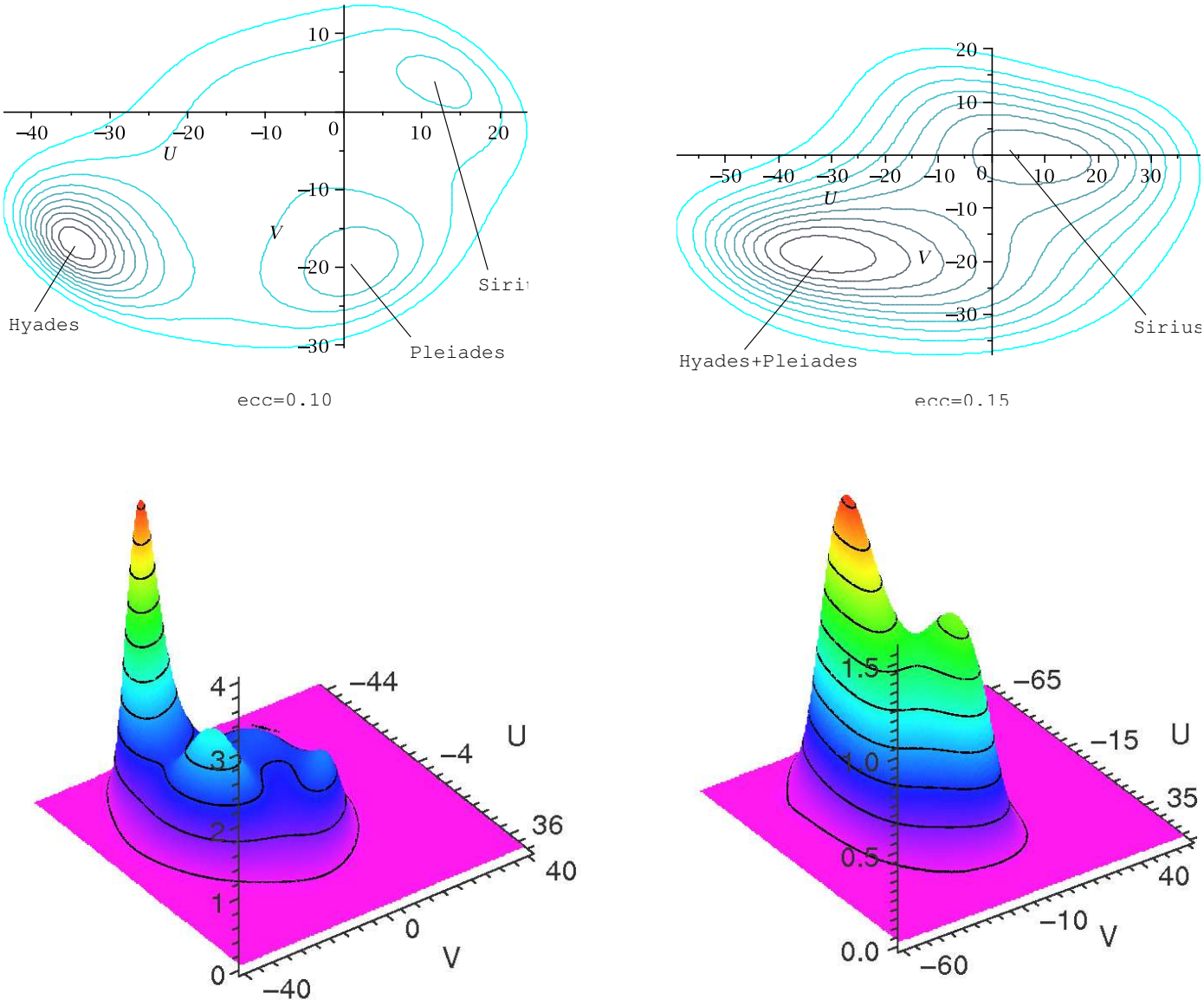

Figure 3: Series of contour plots and distributions on the UV plane for GCS subsamples selected from $|z_{\max}| < 0.5$ kpc and eccentricities up to 0.10 and 0.15.

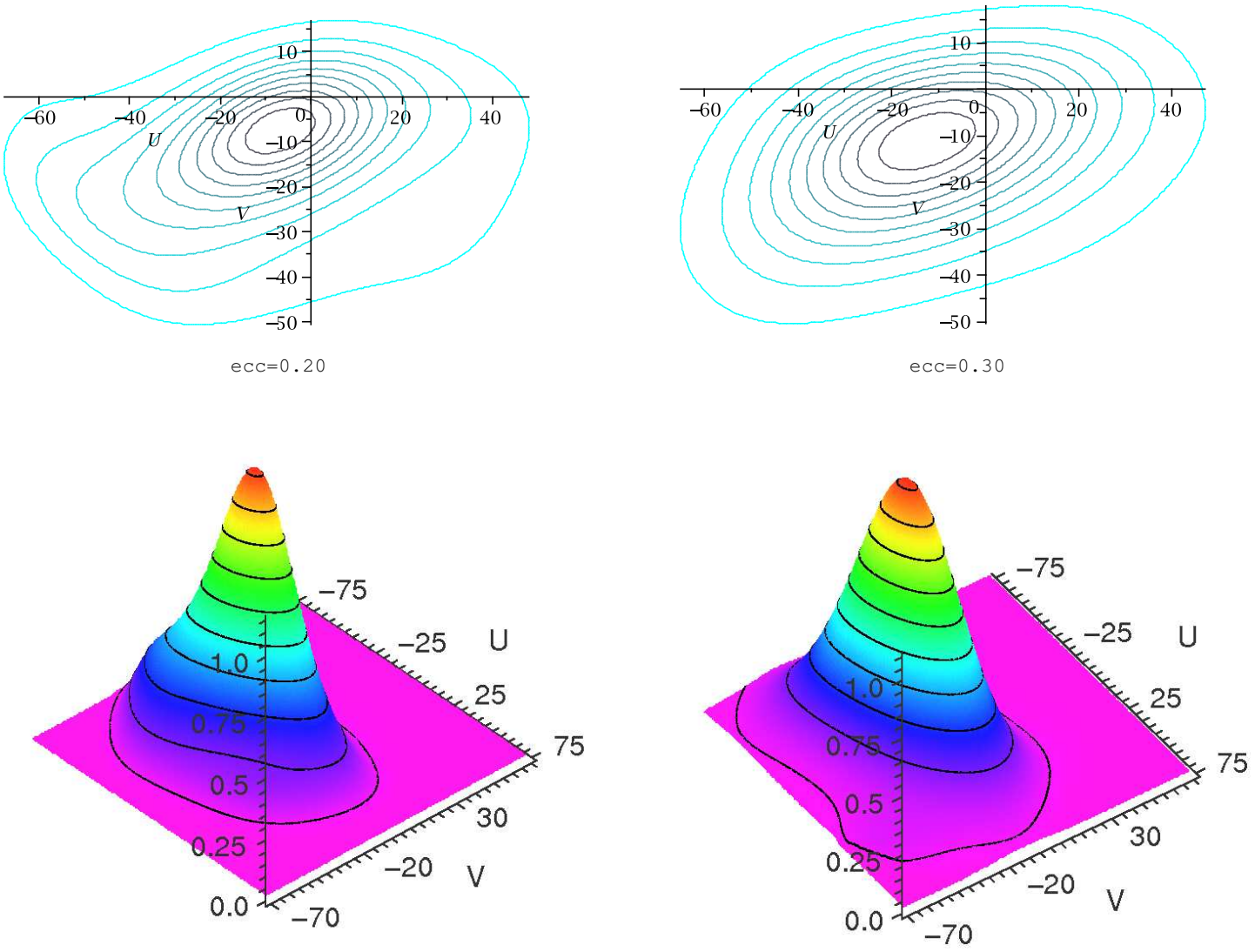

Figure 4: Series of contour plots and distributions on the UV plane for GCS subsamples selected from $|z_{\max}| < 0.5$ kpc and eccentricities up to 0.20 and 0.30.

the vertical motion becomes independent of the radial motion, the motion of a star can be studied as a case of epicyclic orbit. Let us remember that, if a nearly planar orbit is projected onto the Galactic plane, its distance to the Galactic centre oscillates between two limiting values R_p and R_a. The planar eccentricity e is then defined as

$$e = \frac{R_\mathrm{a} - R_\mathrm{p}}{R_\mathrm{a} + R_\mathrm{p}}, \tag{1}$$

which is a dimensionless measure of the deviation from the circular motion in the plane of symmetry.

The orbits in the Galactic disc are nearly planar, and their planar eccentricities may be significantly different from zero (Vidojević & Ninković 2009). Thus, the epicyclic approximation can be used for the current disc sample (Paper II). It is commonly assumed that moving groups of young stars are born in nearly circular orbits (e.g. Dehnen 1998) and, with age, they are transformed into more eccentric orbits, which oscillate locally around the LSR (assumed to be in circular motion, $U_\mathrm{LSR} = 0$, for steady state and axisymmetric systems). Thus, the radial velocity of a star oscillating around the LSR with a period T may be written as

$$U = a \sin \frac{2\pi t}{T}, \tag{2}$$

where the amplitude is proportional to the eccentricity, $a = \frac{2\pi}{T}(R_\mathrm{a}+R_\mathrm{p})\, e$. If the time t is measured in oscillation periods, we may assume $T = 1$.

For a sufficiently great t, e.g., taking several periods, we may also assume that t is uniformly distributed within the interval $[0, 1]$, so that its probability density function is $f_t(t) = 1$, $t \in [0, 1]$, and zero otherwise. We may ask for the distribution of U around the LSR velocity, that is, for the probability of finding a star velocity at any given value within $[-a, a]$. Since $t(U) = \frac{1}{2\pi} \arcsin(\frac{U}{a})$, and this is a two-valued function, the probability density function $f_U(U; a)$, for a given amplitude a, is easily obtained as $2\, f_t(t)\, |t'(U)|$. Thus,

$$f_U(U; a) = \frac{1}{\pi} \frac{1}{\sqrt{a^2 - U^2}}, \quad U \in [-a, a], \tag{3}$$

and zero out of this interval. As seen in Fig. 4 (b), for an arbitrary value $a = 1$, it is less probable to find the star with nearly zero velocity, which means near the extreme positions R_p or R_a, than around the mean position $(R_\mathrm{p} + R_\mathrm{a})/2$ with maximum absolute velocity, either negative by going toward the Galactic centre or positive toward the anticentre.

We may think of a mixture of stars with the same oscillation period and different eccentricities, from zero eccentricity and amplitude, $a = 0$, up to greater amplitudes, say $a = A$. Let us assume a normalised density function $\rho(a)$ of stars in terms of the amplitude a. Then the cumulative density function $h_U(U; A)$ is obtained by integration over a as

$$h_U(U; A) = \int_0^A f_U(U; a)\, \rho(a)\, da. \tag{4}$$

Depending on how the stars are distributed in terms of the amplitude, we may get different symmetric distributions around the LSR. For a fixed period T, this depends on the distribution of eccentricity. The distribution of eccentricity is approximately lognormal, similar to the distribution of wealth in a country, as shown in Fig. 5 from the histogram for the GCS sample, where the interval $[0, 1]$ of eccentricities is divided into 50 bins on the x-axis ($x = 50\, e$ is approximately lognormal with $m = 1.75$ and $\sigma = 0.5$).

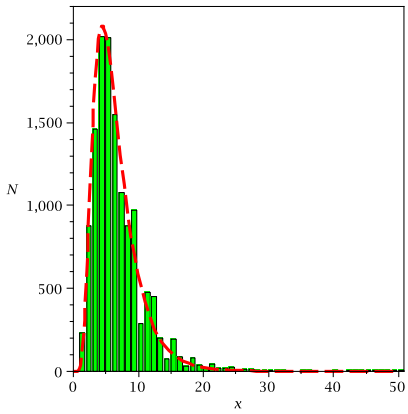

Figure 5: Distribution of eccentricities for the GCS sample. The probability density function obtained from the histogram is approximately lognormal. In the x-axis, the interval $[0, 1]$ of eccentricities is divided into 50 bins. The variable $x = 50\,e$ is lognormal with $m = 1.75$ and $\sigma = 0.5$ (red dashed line).

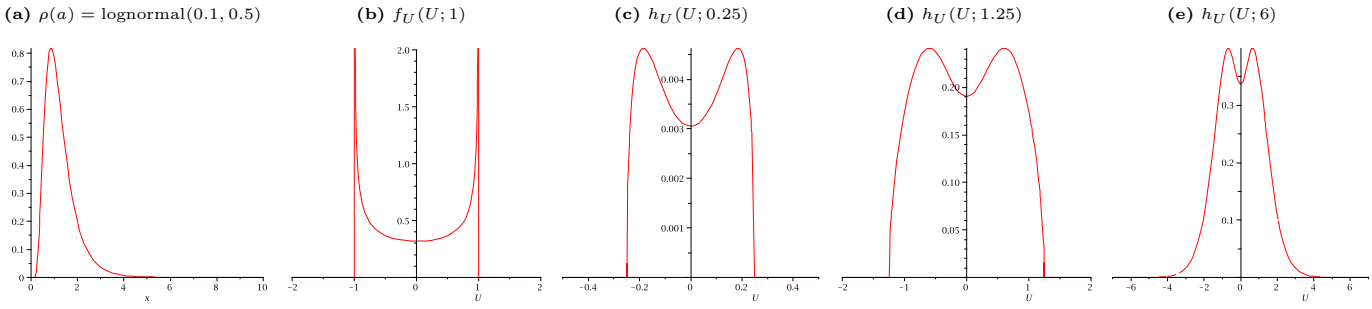

Figure 6: Simulated distribution of radial velocities for arbitrary values of the amplitude, by assuming the epicyclic approximation and $\rho(a)$ lognormal. Bimodal distributions around the origin (LSR) are obtained. (a) Probability density function $\rho(a)$, assumed to be lognormal(0.1,0.5). (b) Probability density function $f_U(U; a)$ for amplitude $a = 1$. (c) Cumulative density function $h_U(U; A)$ integrated up to $A = 0.25$. (d) Cumulative density function $h_U(U; A)$ integrated up to $A = 1.25$. (e) Cumulative density function $h_U(U; A)$ integrated up to $A = 6$.

To find out the shape of $h_U(U;A)$ for a group of stars with the same period, several simulations are carried out for arbitrary values of the amplitude, by assuming $\rho(a)$ lognormal. Bimodal distributions around the origin (LSR) are always obtained, like the plots (c), (d), and (e) of Fig. 6. The mathematical reason is that the lognormal distribution vanishes in a neighbourhood of zero. (It is tangent to zero at the origin.) However, the wider the distribution wing, the less significant the bimodality, since the behaviour for low amplitudes becomes a smaller structure when larger amplitudes are considered. The distribution tends to be Gaussian. In the case of a discrete mixture of stars with different periods, we should get a mixture of densities $h_U(U;A)$ with similar properties, which could explain the radial velocity shape obtained for the inner thin disc. However, for a continuous mixture of populations in terms of oscillation periods, the bimodal structure may be irrelevant. For example, apart from statistical fluctuations, as increasing T, the density function $\rho(a)$ may become more populated around zero, so that it is no longer tangent to zero at the origin of amplitudes. Then, a high-peaked $h_U(U;A)$ may be obtained at the origin, for low values of A. In general, if in a neighbourhood of the origin, $\rho(a)$ behaves as a^p, with $0 < p \leq 1$ we then get smooth unimodal distributions centred at the origin. On the other hand, it is easy to prove that, if the radial velocity does not oscillate symmetrically around the LSR meaning a slight deviation from the epicyclic approximation, the peaks of $h_U(U;A)$ become non-symmetric around the LSR. Therefore, these simple simulations reproduce the actual situation for low eccentricities approximately.

4 Velocity ellipsoids

As a result, the thin disc contain two major streams moving with opposite radial directions around the LSR, one with small positive radial mean velocity and rotation similar to the Sun, and the other with negative radial mean velocity and lower rotation. For each subsystem, we could assume some less restrictive hypotheses, such as point-axial symmetry (opposite points through an axis, allowing, in particular, spiral structures) or a time-dependent model, in order to describe the non-vanishing radial velocity of their centroids and the vertex deviation of their approximate velocity ellipsoids. Thus, a general Chandrasekhar point-axial model (Sanz-Subirana & Català-Poch 1987, Juan-Zornoza et al. 1990, Juan-Zornoza 1995) should be the simplest approximation, where, despite the non-cylindrical symmetry of the system, the solution of Chandrasekhar's equations system yields an axisymmetric potential. In this case, it is interesting to recall the relationship between the vertex deviation and the radial mean velocity.

It is well known that the vertex deviation δ of a velocity ellipsoid depends on the second central moments in the form

$$\tan(2\delta) = \frac{2\mu_{UV}}{\mu_{UU} - \mu_{VV}}. \tag{5}$$

Thus, if $\mu_{UU} - \mu_{VV} > 0$, the angle δ and the moment μ_{UV} have the same sign. As explained in Cubarsi & Alcobé (2006), the radial mean velocity referred to an axisymmetric (cylindrical) system can be related to the increment of rotation mean velocity with respect to the same axisymmetric system and, in particular, to the vertex deviation of the velocity ellipsoid, through the expression

$$U_0 - U_0^{(\mathrm{cyl})} = \frac{\mu_{UV}}{\mu_{VV}}\,\Theta_0 \tag{6}$$

where U_0 is the radial mean velocity, $U_0^{(\mathrm{cyl})}$ the radial mean velocity of an ideal axisymmetric system (which is now associated with the LSR), and Θ_0 the galactocentric rotation mean velocity. This is not a special situation, and recent studies of the shape of velocity ellipsoids in spiral galaxies

Table 1: Distribution parameters for HIPPARCOS and GCS samples with radial velocity errors up to 2.5 km s^{-1} (Samples I', II', III', and IV' from Cubarsi (2009)). The last sample contains representative thin disc stars, obtained from eccentricities $e \leq 0.3$ and $|z_{\max}| \leq 0.5$ kpc. The displayed parameters are dispersions σ_U, σ_V, σ_W, vertex deviation δ on the UV-plane, curtosis c_U, c_V, c_W, and skewness γ_U, γ_V, γ_W.

Sample	σ_U	σ_V	σ_W	δ [°]	c_U	c_V	c_W	γ_U	γ_V	γ_W
HIP total	36.2 ±0.6	30.8±1.0	18.6±0.5	7.6±6.6	9.3 ±4.0	37.0 ±13.9	20.7 ±14.8	0.2 ±0.2	-4.5 ±0.8	-0.9 ±0.5
$\|\mathbf{V}\| \leq 51$	19.9 ±0.1	13.2 ±0.1	10.7 ±0.1	12.3 ±0.8	-0.4 ±0.1	0.1 ±0.3	1.5 ±0.5	0.3 ±0.0	0.2 ±0.0	0.2 ±0.1
GCS total	35.2 ±0.4	26.1 ±0.6	18.6 ±0.5	10.7 ±2.4	5.5 ±2.8	22.7 ±9.3	35.2 ±42.4	-0.1 ±0.2	-3.1 ±0.5	-0.9 ±1.0
$\|\mathbf{V}\| \leq 51$	21.5 ±0.1	14.1 ±0.1	12.4 ±0.1	8.7 ±0.6	-0.7 ±0.1	0.0 ±0.2	0.7 ±0.3	0.2 ±0.0	0.2 ±0.0	0.1 ±0.0
$e \leq 0.3$	29.1 ± 0.2	18.1 ± 0.1	11.6 ± 0.1	9.6 ±0.6	0.2 ±0.2	0.4 ±0.2	-0.4 ±0.1	0.1 ±0.0	-0.3 ±0.0	0.0 ±0.0

(Vorobyov & Theis 2008) confirm that the magnitude of the vertex deviation is not correlated with the gravitational potential (even though it is assumed non-axisymmetric), but is strongly correlated with the spatial gradients of the mean stellar velocities, in particular with the radial gradient of the mean radial velocity.

Thus, according to Eq. 6, a velocity ellipsoid with a positive [negative] vertex deviation might be associated with a loss of axisymmetry and with a radial motion towards [against] the Galactic centre.

In Fig. 7 (left) the two major stellar groups with opposite radial velocities around the LSR, which support the largest structure within the thin disc, are associated with two velocity ellipsoids with similar total dispersions. The one moving toward the Galactic centre, with radial and rotation galactocentric mean velocities $U_0 = 15, \Theta_0 = 220$, and the other one, toward the anticentre, with mean motion $U_0 = -15, \Theta_0 = 200$. The LSR is placed in the middle of both ellipsoids in a similar situation to the sample with maximum eccentricity 0.15. By assuming the same mixture proportions $n' = n''$, the partial diagonal central moments $\mu'_{ii} = \mu''_{ii}$ are obtained from totals and from their deferential mean velocity $u'_i - u''_i$, from the usual relationship

$$\mu_{ii} = n'\mu'_{ii} + n''\mu''_{ii} + n'n''(u'_i - u''_i)^2; \quad i = 1, 2, 3. \tag{7}$$

The vertex deviation of each ellipsoid is obtained from Eq. 6. The total moments are taken from the sample with maximum eccentricity $e = 0.3$. The graph shows the partial ellipsoids $\mathbf{u}^{\mathrm{T}} \cdot \mu_2^{-1} \cdot \mathbf{u} = 1$, in blue, and the thin disc velocity ellipsoids $\mathbf{u}^{\mathrm{T}} \cdot \mu_2^{-1} \cdot \mathbf{u} = 2, 3$, in red. The ellipsoid with positive radial velocity has a positive vertex deviation (although small), and the one with negative radial peculiar velocity has negative vertex deviation (also small). The shape of the thin disc, in particular its apparent positive vertex deviation, is generated from the inner structure. The green dashed partial ellipsoids represent a situation with the opposite radial motions, so that, in such a case, the apparent total vertex deviation should be negative. On the right, the contour plots in the UV plane (in heliocentric velocities) for the samples with maximum eccentricity $e = 0.15$ (blue) and $e = 0.3$ are superposed. Simulated and actual plots are totally consistent.

5 Conclusions

In addition to limited velocity distributions, in Cubarsi (2009) other truncated distributions were analysed in terms of metallicity, colour, maximum distance to the Galactic plane, and eccentricity. Those star properties were correlated with the star's expected population obtained in Paper II. The only significant correlations that are maintained within thin disc stars are the absolute velocity and the eccentricity, since metallicity and $|z_{\max}|$ are more appropriate for segregating thick disc

and halo stars from the thin disc. In particular, the eccentricity, which is directly related to the isolating integrals of the star motion, is more discriminating than the absolute velocity for selecting subsamples. However, a part of thin and thick disc stars may have similar eccentricities. Then, to isolate thin disc stars, it is necessary to combine two sampling parameters: eccentricity and $|z_{\max}|$. A representative thin disc, containing 90% of the whole sample, is selected from maximum eccentricity 0.3 and $|z_{\max}| \leq 0.5$ kpc. Its central moments are similar to the ones obtained for the thin disc in Paper II. Some characteristic parameters of the distribution are compared in Table 1. Furthermore, within the thin disc sample, the eccentricity behaves as an excellent sampling parameter that distinguishes between different eccentricity layers allowing subjacent structures to be visualised.

For subsamples obtained from eccentricities $e < 0.15$, the maximum entropy method is able to plot the classical moving groups composing the small-scale structure of the velocity distribution, as described from other algorithms based on an arbitrary number of mixture components, wavelet transforms, or maximum likelihood (e.g., Famaey et al. 2007, Veltz et al. 2008, Skuljan et al. 1999, Dehnen 1998), especially those providing a modest amount of complexity (Bovy et al. 2009). For these subsamples with small eccentricities, there is a general trend: the star velocities are approximately symmetrically distributed around the LSR in the radial direction. In most cases the distribution is bimodal, with a dearth of stars at the LSR. At the end, for $e = 0.15$, the core distribution of the thin disc is supported by two major stellar groups with opposite radial velocities, referred to the LSR. One bulk, with zero or small positive heliocentric radial mean velocity, has a lower peak but a wider distribution around Sirius/UMa stream. The other one, with radial velocity about -30 km s^{-1}, has mean rotation ≈ -20 km s^{-1} and a higher peak, containing the main groups Hyades and Pleiades.

For stars with a similar period of oscillation around the LSR in the radial direction (under the epicyclic approximation), several simulations allow us to confirm that such a two-peaked distribution of radial velocities is due to a lognormal distribution of the eccentricities. For a mixture of stars with different periods and a lognormal distribution of the velocity amplitude of the stellar orbits, the bimodal shape is maintained. However, if the number of stars with nearly vanishing amplitude increases, then the radial velocity distribution becomes unimodal, similar to the total thin disc sample with $e = 0.3$.

The bimodal behaviour of the central disc associated with the previous major subsystems may then be explained from two different phenomena. On one hand, it may be a perturbation similar to a pressure wave acting in part along the radial direction that induces an oscillation of the radial velocity around the LSR. Let us remember that the oscillation of each subsystem centroid along the U direction is also the expected motion of axisymmetric systems under steady state potentials (e.g. Cubarsi et al. 1990). On the other hand, both kinematical major groups, which actually are placed at the solar position, are in opposite oscillation states. In addition both groups have a difference of about 20 km s^{-1} in rotation mean velocity, so that one group of stars actually surpasses the other group. Therefore, the apparent vertex deviation of the thin disc may stem from the swinging of those major kinematic groups. A scenario of a continuously changing orientation of the disc pseudo ellipsoid is then possible.

References

Bovy J., Hogg D.W., Roweis S.T. 2009, ApJ, 700, 1794

Cubarsi R., Sanz J., Juan J.M. 1990, Ap&SS 170, 197

Cubarsi R., Alcobé S. 2006, A&A 457, 537

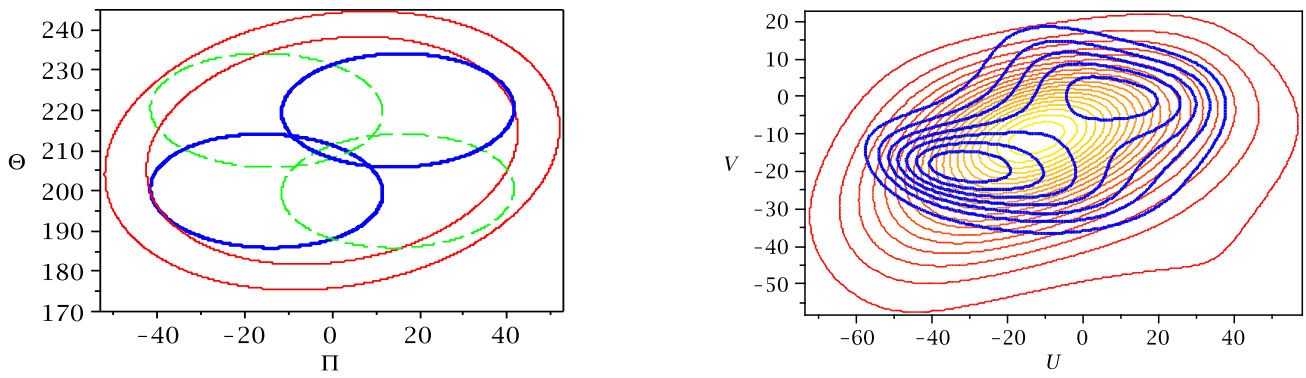

Figure 7: (Left) Velocity ellipsoids, in blue, depicted according to Eqs. 6 and 7, from total moments corresponding to the sample with eccentricities $e \leq 0.3$. They are centred in galactocentric velocities $\Pi_0 = 15, \Theta_0 = 220$, and $\Pi_0 = -15, \Theta_0 = 200$, with the LSR placed in the middle of them. Thin disc isocontours, in red, with positive vertex deviation, are generated from the inner structure. The green dashed partial ellipsoids represent a situation with the opposite radial motions. (Right) Contour plots in the UV plane (heliocentric velocities) for the samples with maximum eccentricity $e = 0.15$ (blue) and $e = 0.3$ (red).

Cubarsi R. 2008, On the maximum entropy and the problem of moments: an application to stellar kinematics. Universitat Politecnica de Catalunya, Barcelona. E-prints http://hdl.handle.net/2117/XXXX

Cubarsi R. 2009, Structure of the velocity distribution of the Galactic disc. The maximum entropy statistical approach - Part I. Universitat Politecnica de Catalunya, Barcelona. E-prints http://hdl.handle.net/2117/3046

Cubarsi R., Alcobé S., Vidojević S., Ninković S. 2009, A&A http://dx.doi.org/10.1051/0004-6361/200912818

Dehnen W. 1998, AJ 115, 2384

Dehnen W., Binney J.J. 1998, MNRAS, 298, 387

Famaey B., Jorissen A., Luri X., Mayor M., Udry S., Dejonghe H., Turon C. 2005, A&A 430, 165

Famaey B., Pont F., Luri X., Udry S., Mayor M., Jorissen, A. 2007, A&A 461, 957

Juan-Zornoza J.M., Sanz-Subirana J., Cubarsi R. 1990, Ap&SS, 170, 343

Juan-Zornoza J.M. 1995, PhD. Thesis. ISBN: 84-475-0767-X (Barcelona: Universitat de Barcelona)

Nordström B., Mayor M., Andersen J., Holmberg J., Pont F., Jørgensen B.R., Olsen E.H., Udry S., Mowlavi N. 2004, A&A 418, 989

Sanz-Subirana, J., Català-Poch, M.A. 1987, in 10th ERAM of the IAU, volume 4, 267

Skuljan J., Hearnshaw J.B., Cottrell P.L. 1999, MNRAS 308, 731

Veltz et al. 2008, A&A 480, 753

Vidojević S., Ninković S. 2009, AN, 330, 46